Effects of environmental stressors on daily governance

Supplementary Information

Nick Obradovich[*]*, Dustin Tingley, and Iyad Rahwan*

Contents

[*]Corresponding author, nobradov@mit.edu.

List of Figures

List of Tables

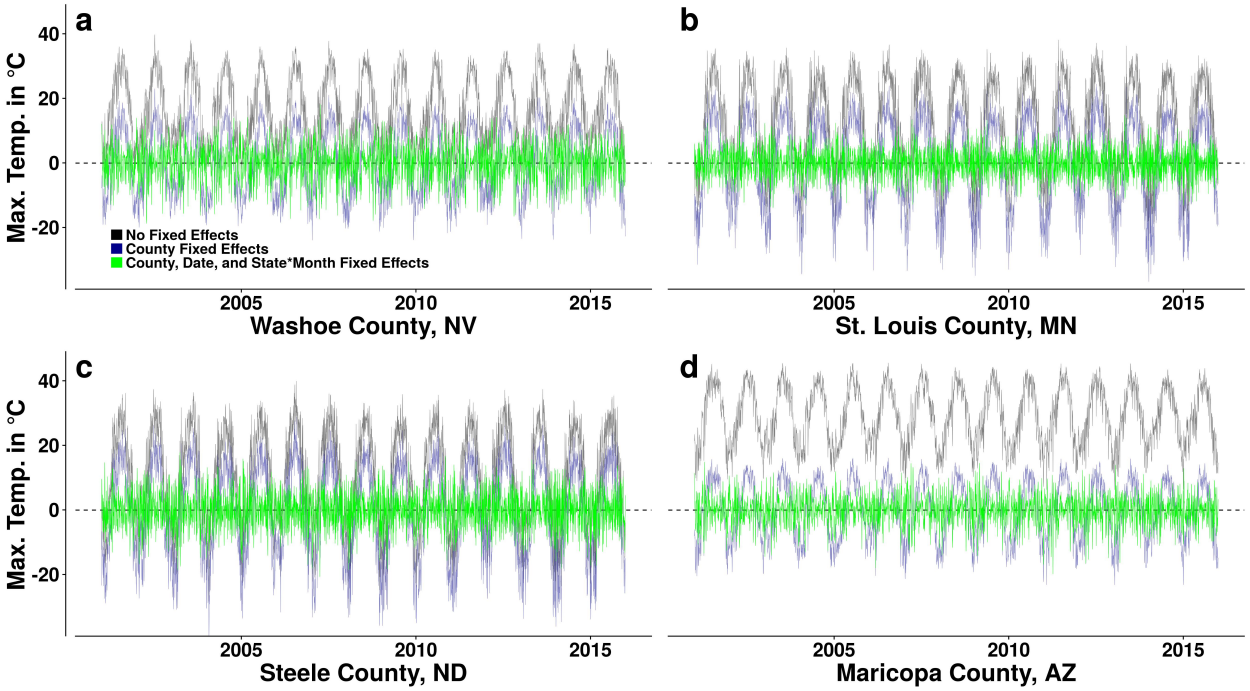

Fig. S1. Deconvolved daily temperature variation. Each panel of this figure depicts three series. The first is the raw daily temperature observations, the second is the remaining temperature variation after deconvolving the raw data around county-level fixed effects, the third is the remaining variation after deconvolving the raw data around our full set of county, date, and state-by-calendar-month fixed effects. As can be seen, the remaining variation after deconvloving the fixed effects is stationary across both seasons and years. Panel (a) plots this relationship for Washoe County, NV. Panel (b) plots this relationship for St. Louis County, MN. Panel (c) plots this relationship for Steele County, ND. Panel (d) plots this relationship for Maricopa County, AZ.

Deconvolved temperature

Fig. S1 displays the effect of deconvolving the raw daily temperature series around unit as well as unit, date, and state-by-calendar-month fixed effects (1, 2). As can be seen, seasonal and long-term trends are removed and the remaining identifying variation is stationary (3) (not systematically trending over time) and centered around zero for each individual unit.

Marginal effects

Fig. S2 displays the marginal effects associated with the quadratic estimates from the main text results (4). Each estimated relationship has substantial portions of its marginal effects' confidence intervals that do not contain zero. Of note, the negative marginal effects for the colder portion of the number of violations per inspection relationship are estimated with high uncertainty, while the higher temperature portion of the distribution returns increasingly positive marginal effects estimated with higher statistical precision. Panel (a) of Fig. S2 draws from the estimates presented in model (1) of Table S1. Panel (b) of Fig. S2 draws from the estimates presented in model (1) of Table S2. Panel (c) of Fig. S2 draws from the estimates presented Table S3. Panel (d) of Fig. S2 draws from the estimates presented in model (2) of Table S5.

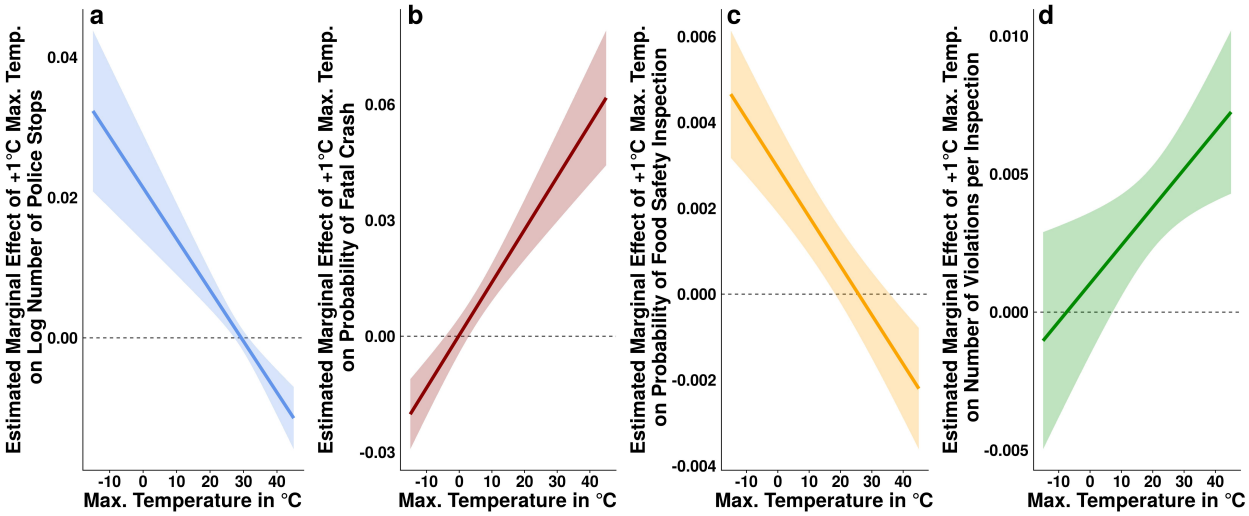

Fig. S2. Marginal effects and confidence intervals of quadratic estimates. This figure plots the marginal effects of the quadratic estimates from the main text. Panel (a) plots the marginal effect of a one degree increase in maximum temperature on the log number of police stops. Panel (b) plots the marginal effect of temperature on the probability of a fatal crash. Panel (c) plots the marginal effect of temperature on the probability of a food safety inspection. Panel (d) plots the marginal effect of temperature on the number of food safety violations per inspection. Shaded regions plot the 95% confidence intervals of the marginal effects.

Flexible functional forms

Fig. S3 displays the marginal effects from estimating $f()$ from the main text using flexible non-parametric bins of maximum temperature rather than our quadratic parametric functional form in the main text (5–10). The first bin contain the portion of the temperature distribution from $-\infty$ to -10 and the last bin contains 40 to ∞. As can be seen, the functional forms recovered by our non-parametric approach recover functional forms that approximate those recovered by our quadratic estimation of $f()$ in the main text. Because of the over one billion facility-days in our disaggregated facility-level analysis and due to the added columns required to estimated the binned functional form, we are unable to estimate the binned regression on the facility-level data. Thus, for this estimation we aggregate our facility-level data up to the county-level and employ our county-level estimation strategy. This aggregation procedure returns similar functional forms as uncovered in our county-aggregated inspections and violations regressions, presented in *SI: County-aggregated inspections* and *SI: County-aggregated violations* sections below.

Examination of potential targeting

Fig. S4 depicts the results of stratifying our sample of facilities into quartiles by their total numbers of food safety violations over the course of our sample. The first quartile represents facilities with lower numbers of violations while the fourth quartile represents higher risk facilities. If higher temperatures drove substitution of regulatory effort away from greater numbers of low-risk inspections towards smaller numbers of high-risk facilities, then we would expect to see reductions in inspections due to high temperatures for the first and second quartile of facilities and increases in inspections due to high temperatures for the third and fourth quartiles. However, across all four quartiles we observe functional forms that mirror those estimated in the main text. Across all types of facilities, hot temperatures reduce the probability of food safety inspection.

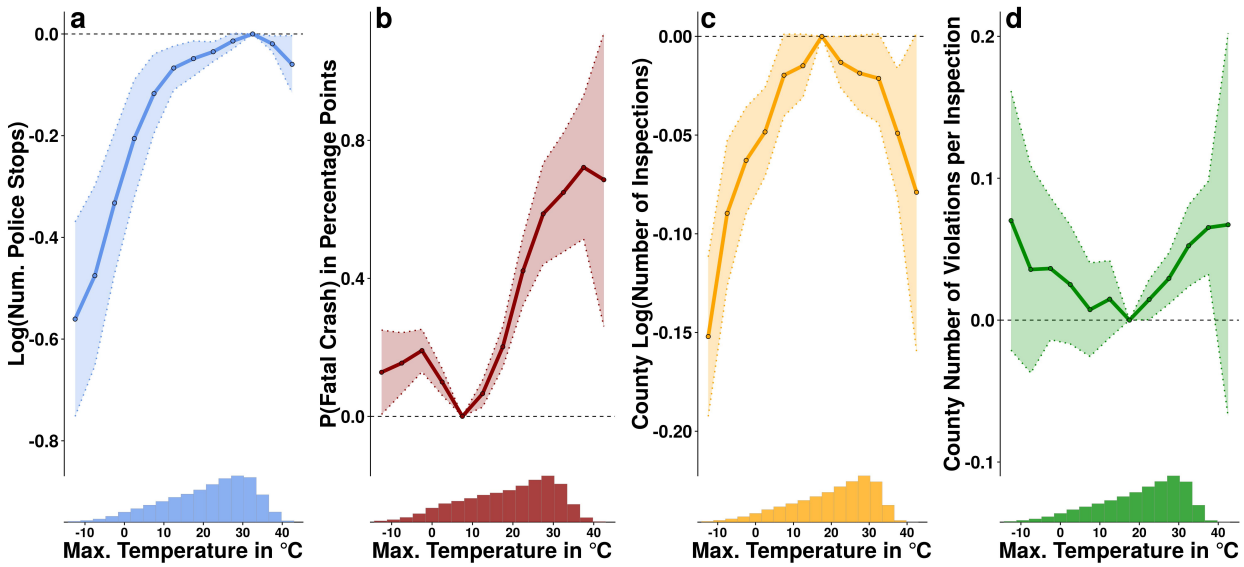

Fig. S3. Binned maximum temperatures for estimating $f()$. This figure plots the marginal effects estimated from binning maximum temperatures into 5°C bins. Y-axes report the estimated change in each respective outcome variable as compared to the omitted temperature bin in each relationship. For each estimation, we omit the bin containing the extremum for that relationship. Panel (a) plots the marginal effect of maximum temperature on the log number of police stops. Panel (b) plots the marginal effect of maximum temperature on the probability of a fatal crash. Panel (c) plots the marginal effect of temperature on the county-aggregated, log number of food safety inspections. Panel (d) plots the marginal effect of temperature on the county-day average number of food safety violations per inspection. Shaded regions plot the 95% confidence intervals of the estimated marginal effects.

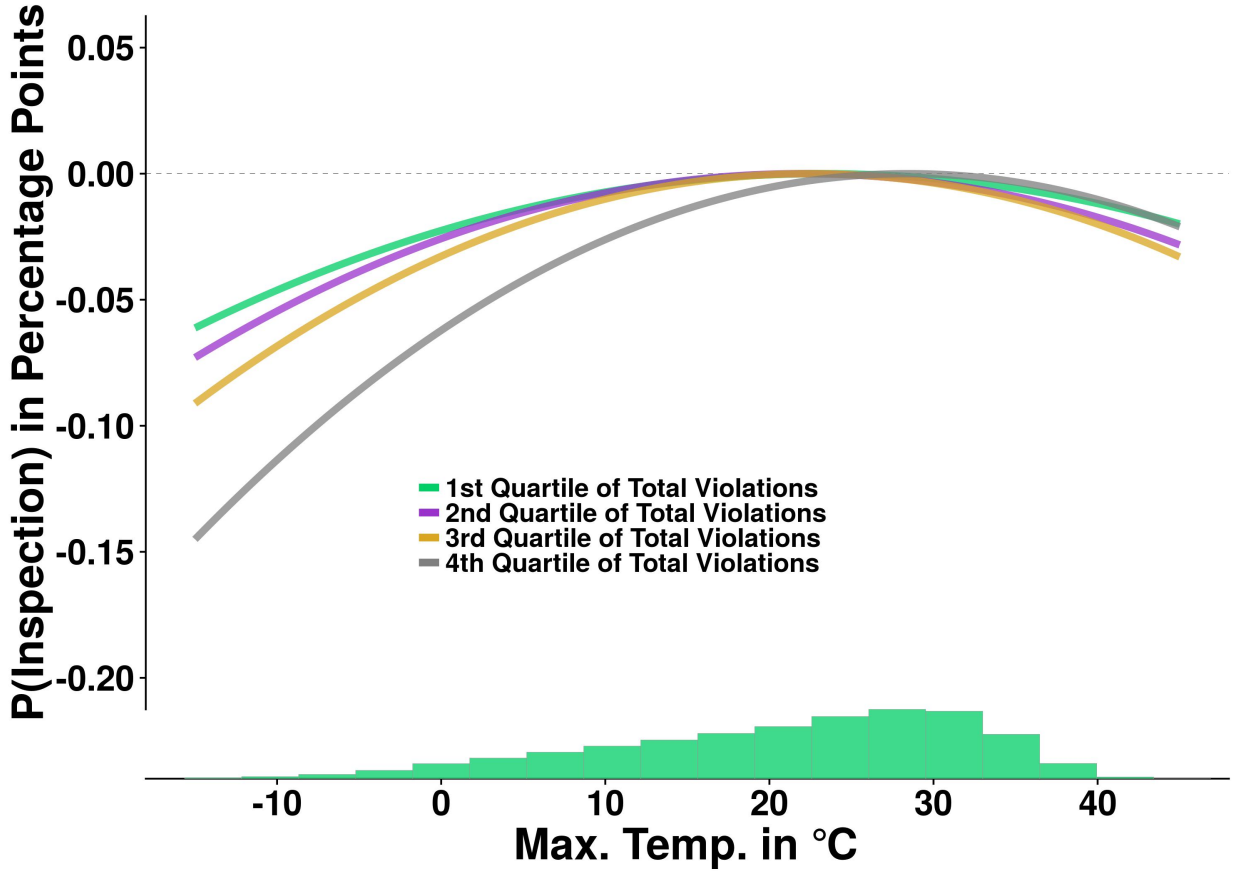

Fig. S4. Examination of possible substitution of inspection effort from low risk to high risk facilities. This figure plots the effects of maximum temperatures on the probability of food safety inspection across quartiles of total violations by facility. This estimation follows the same procedure as in the main text Fig. 3a, but represents separately estimating the regression for each quartile of total food safety violations by facility. The first quartile represents facilities with the lowest numbers of violations in our sample while the fourth quartile represents the facilities with the highest number of violations. As can be seen, the effects of hot temperatures on probability of inspection are negative across each quartile, suggesting that there is no substantial redirection of regulatory effort from low-risk violators to high-risk violators as a function of maximum temperatures. Each relationship is significant at the $p < 0.001$ level.

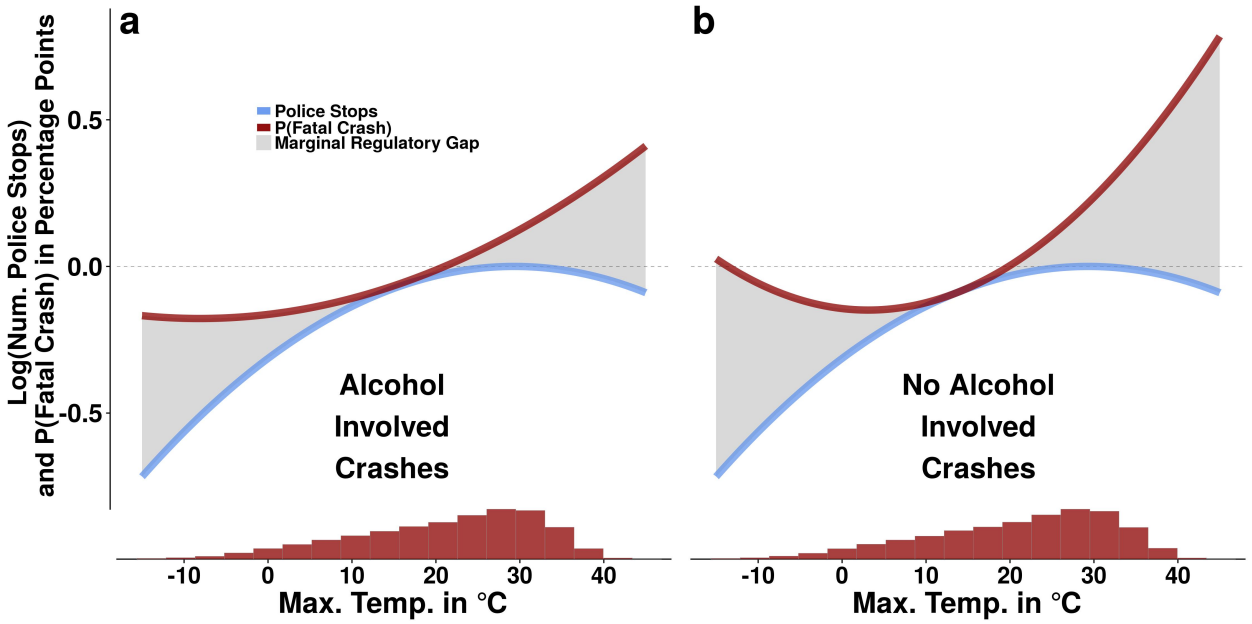

Fig. S5. Alcohol involved versus no alcohol involved crashes as a function of maximum temperatures. This figure plots the same police stops functional form as in the main text, with separate estimates of the fatal crash and maximum temperature functional form. Panel (a) estimates the effect of maximum temperatures on the probability of fatal crashes where alcohol was involved. Panel (b) estimates the effect of maximum temperatures on the probability of fatal crashes where no alcohol was detected. The relationship for no alcohol involved crashes is steeper than for no alcohol involved crashes, though each relationship is significant at the $p < 0.001$ level.

Alcohol involved crashes

Fig. S5 depicts the comparative effects of maximum temperatures on the probability of alcohol involved versus no alcohol involved fatal crashes (11). Crashes where no alcohol was detected or suspected of being involved see more steep increases in response to high temperatures than crashes where alcohol was suspected, suggesting that fatigue (12) or cognitive impairment directly due to heat (13) may play a more substantial role in mediating the relationship as compared to ancillary behavioral changes (more alcohol ingestion), though these suggestive results require further investigation. Table S2, in models (3) and (4), displays the regression results of this estimation.

Regression tables

We include the regression tables associated with each of our analyses below. Because of our substantial number of fixed effects for each model, we estimate our models using the *felm()* function from the *lfe* package in the **R** statistical programming language.

Police stops

Table S1. Police Stops Regression Table

	Dependent Variable: Log Number of Stops			
	Restricted	Restricted	Full	Full
	(1)	(2)	(3)	(4)
TMAX	0.021***		0.018***	
	(0.004)		(0.003)	
TMAX^2	−0.0004***		−0.0003***	
	(0.0001)		(0.0001)	
HEAT INDEX		0.014***		0.012***
		(0.002)		(0.002)
HEAT INDEX^2		−0.0002***		−0.0001***
		(0.00002)		(0.00002)
PRCP	−0.012***	−0.012***	−0.011***	−0.011***
	(0.001)	(0.001)	(0.001)	(0.001)
TRANGE	0.001	0.002	0.002	0.003***
	(0.001)	(0.001)	(0.001)	(0.001)
CLOUD	−0.002***	−0.002***	−0.002***	−0.002***
	(0.0003)	(0.0003)	(0.0002)	(0.0002)
HUMID	−0.001***		−0.001***	
	(0.0003)		(0.0002)	
WIND	−0.005**	−0.005**	−0.004***	−0.005***
	(0.002)	(0.002)	(0.001)	(0.001)
County FE	Yes	Yes	Yes	Yes
Date FE	Yes	Yes	Yes	Yes
State:Month FE	Yes	Yes	Yes	Yes
Observations	938,273	938,273	2,382,876	2,382,876
R^2	0.722	0.721	0.718	0.718
Adjusted R^2	0.720	0.719	0.717	0.717
Residual Std. Error	0.551	0.552	0.727	0.727

Note: *p<0.01; **p<0.005; ***p<0.001
Standard errors are in parentheses and are clustered on state.

Table S1 displays our regressions for the relationship between meteorological variables and the log number of police stops in a county-day. Model (1) plots the relationship depicted in the main text, while model (2) substitutes the heat index (14, 15) for maximum temperature and relative humidity. The results are similar between maximum temperatures and the heat index: at low and high portions of each distribution the log

number of police stops declines. Models (1) and (2) employ counties with less than thirty days of zero stops over the full sample from all states that report county and date of stop in the data. These counties contain 74 percent of all the stops in the full data. Models (3) and (4) of Table S1 expand the sample of counties to all county-days with stops in the data, and include stops from counties with sparser reporting of stops, adding the remaining 26 percent of stops to the analysis. As can be seen, even including these smaller counties' observations in the sample, the estimated relationships are quite similar.

Fatal crashes

Table S2. Fatal Crashes Regression Table

	Dependent Variable: Fatal Crash (0/1)			
	Full	Full	Alcohol	No Alcohol
	(1)	(2)	(3)	(4)
TMAX	0.0003		0.003*	−0.003
	(0.002)		(0.001)	(0.002)
TMAX²	0.001***		0.0002***	0.001***
	(0.0001)		(0.0001)	(0.0001)
HEAT INDEX		0.007**		
		(0.002)		
HEAT INDEX²		0.0001		
		(0.00003)		
PRCP	0.005***	0.005***	−0.001***	0.007***
	(0.001)	(0.001)	(0.0003)	(0.001)
TRANGE	0.001	0.011***	0.001	0.0001
	(0.002)	(0.002)	(0.001)	(0.002)
CLOUD	−0.001	−0.001	−0.001***	−0.0001
	(0.0004)	(0.0004)	(0.0002)	(0.0003)
HUMID	−0.002***		−0.001***	−0.001**
	(0.0004)		(0.0002)	(0.0003)
WIND	−0.009***	−0.007**	−0.006***	−0.004
	(0.002)	(0.002)	(0.001)	(0.002)
County FE	Yes	Yes	Yes	Yes
Date FE	Yes	Yes	Yes	Yes
State:Month FE	Yes	Yes	Yes	Yes
Observations	17,022,516	17,022,516	16,710,930	16,858,888
R^2	0.086	0.086	0.056	0.058
Adjusted R^2	0.085	0.085	0.055	0.057
Residual Std. Error	15.754	15.755	9.573	13.077

Note: *p<0.01; **p<0.005; ***p<0.001
Standard errors are in parentheses and are clustered on state.
Probability is reported in percentage points.

Table S2 displays our regression results for linear probability model of the relationship between weather and the incidence of fatal crashes. Model (1) plots the relationship depicted in the main text, while model (2) substitutes the heat index for maximum temperature and relative humidity. The marginal effects from model (2) indicate that the risk of fatal crash is also increased by high observations of the heat index. Models (3) and (4) of Table S2 plot the relationship between maximum temperatures and fatal crashes for crashes with and without alcohol involved, respectively. See *SI: Alcohol involved crashes* for more details.

Food safety inspections

Probability of food safety inspection

Table S3 displays our regressions for the relationship between meteorological variables and the probability of food safety inspection a facility-day. Model (1) plots the relationship depicted in the main text, while model

Table S3. Probability of Food Safety Inspection Regression Table

	Dependent Variable: Inspection (0/1)	
	(1)	(2)
TMAX	0.003***	
	(0.001)	
TMAX²	−0.0001***	
	(0.00001)	
HEAT INDEX		0.002***
		(0.0005)
HEAT INDEX²		−0.00003***
		(0.00001)
PRCP	−0.0003**	−0.0004***
	(0.0001)	(0.0001)
TRANGE	−0.0005	−0.0003
	(0.0005)	(0.001)
CLOUD	−0.00001	−0.00004
	(0.00002)	(0.00003)
HUMID	−0.0002	
	(0.0001)	
WIND	−0.001	−0.001
	(0.001)	(0.001)
Facility FE	Yes	Yes
Date FE	Yes	Yes
State:Month FE	Yes	Yes
Observations	1,176,731,121	1,176,731,121
R^2	0.004	0.004
Adjusted R^2	0.003	0.003
Residual Std. Error	5.885	5.885

Note: *p<0.01; **p<0.005; ***p<0.001
Standard errors are in parentheses and are clustered on state.
Probability is reported in percentage points.

(2) substitutes the heat index (14, 15) for maximum temperature and relative humidity. The results are similar between maximum temperatures and the heat index: at low and high portions of each distribution the predicted probability of food safety inspection declines.

County-aggregated inspections

Table S4. Log Number of Food Safety Inspections in County

	Dependent Variable: Log Number of Inspections	
	(1)	(2)
TMAX	0.005***	
	(0.001)	
TMAX²	−0.0001***	
	(0.00003)	
HEAT INDEX		0.003***
		(0.001)
HEAT INDEX²		−0.00004***
		(0.00001)
PRCP	−0.0004*	−0.0004
	(0.0002)	(0.0002)
TRANGE	−0.0001	−0.0005
	(0.001)	(0.001)
CLOUD	−0.0001	−0.0002
	(0.0001)	(0.0001)
HUMID	−0.0001	
	(0.0002)	
WIND	−0.001	−0.001
	(0.001)	(0.001)
County FE	Yes	Yes
Date FE	Yes	Yes
State:Month FE	Yes	Yes
Observations	600,160	600,160
R^2	0.880	0.880
Adjusted R^2	0.879	0.879
Residual Std. Error	1.347	1.347
Note:		*p<0.01; **p<0.005; ***p<0.001
	Standard errors are in parentheses and are clustered on state.	
	Regressions are weighted by number of facilities per county.	

As our facility-level model estimates a linear probability model with sparse occurrence of inspections (but allowing for facility-level fixed effects), we examine whether our results are robust to aggregation up to the county-level. Table S4 displays the results of examining the effect of meteorological conditions on log number of food safety inspections. Model (1) examines the effect of maximum temperatures on food safety inspections, finding that – ass in the facility-level model – cold and hot temperatures reduce the log number of food safety inspections. Model (2) observes a similar relationship across the distribution of the heat index.

Food safety violations

Number of violations per inspection

Table S5 displays our regressions for the relationship between meteorological variables and the number of food safety violations conditional upon inspection on a facility-day. Model (1) plots the relationship depicted in the main text, while model (2) substitutes the heat index (14, 15) for maximum temperature and relative humidity. At high portions of the maximum temperature distribution the number of food safety violations per inspection is highest. Marginal effects at colder portions of the temperature distribution are estimated with higher statistical uncertainty (see *SI: Marginal effects* for details). The heat index measure indicates a positive and predominantly linear relationship between added heat index and number of violations.

Table S5. Food Safety Number of Violations Regression Table

	Dependent Variable: Number of Violations per Inspection	
	(1)	(2)
TMAX	0.001	
	(0.001)	
TMAX^2	0.0001*	
	(0.00003)	
HEAT INDEX		0.003*
		(0.001)
HEAT INDEX^2		−0.00001
		(0.00002)
PRCP	0.0003	0.0004
	(0.0004)	(0.0003)
TRANGE	−0.002	−0.002**
	(0.001)	(0.001)
CLOUD	0.0001	0.0001
	(0.0001)	(0.0001)
HUMID	0.001**	
	(0.0002)	
WIND	−0.003***	−0.003***
	(0.001)	(0.001)
Facility FE	Yes	Yes
Date FE	Yes	Yes
State:Month FE	Yes	Yes
Observations	4,101,987	4,101,987
R^2	0.522	0.522
Adjusted R^2	0.414	0.414
Residual Std. Error	2.689	2.689
Note:		*p<0.01; **p<0.005; ***p<0.001
	Standard errors are in parentheses and are clustered on state.	

Probability of violation per inspection

As number of violations per inspection is small on average, we investigate whether our results are robust to bifurcating the variable and running a linear probability model to estimate the effect of meteorological conditions on the probability of any violation conditional upon a food safety inspection. As can be seen in Table S6, the effects of maximum temperatures on probability of food safety inspection mirror those estimated in the number of violations per inspection model. The heat index functional form is similar to that for maximum temperatures, with higher portions of the distribution estimated with lower statistical uncertainty.

County-aggregated violations

As for inspections, we aggregate our violations per inspection up to the county-level from the facility-level. Our outcome measure for these regressions is the mean number of violations per inspection at a county-day. Table S7 displays the results of estimating the effects of meteorological conditions on county-level mean number of violations per inspection. High maximum temperatures substantially increase violations (see model (1)) and high heat index values also increase violations, though this relationship is estimated with lower statistical precision (see model (2)).

Trimmed temperature

One might be concerned that outliers on the temperature distribution – very hot days in hot places and very cold days in cold places – could put undue leverage on our estimated relationships presented in the main text

Table S6. Food Safety Probability of Violation Regression Table

	Dependent Variable: Any Violation (0/1)	
	(1)	(2)
TMAX	−0.020	
	(0.019)	
TMAX²	0.001**	
	(0.0005)	
HEAT INDEX		0.004
		(0.013)
HEAT INDEX²		0.0003
		(0.0002)
PRCP	0.001	0.001
	(0.004)	(0.004)
TRANGE	−0.020	−0.015
	(0.013)	(0.011)
CLOUD	0.001	0.001
	(0.001)	(0.001)
HUMID	0.002	
	(0.003)	
WIND	−0.027	−0.027
	(0.015)	(0.015)
Facility FE	Yes	Yes
Date FE	Yes	Yes
State:Month FE	Yes	Yes
Observations	4,101,987	4,101,987
R^2	0.383	0.383
Adjusted R^2	0.243	0.243
Residual Std. Error	36.486	36.486

Note: *p<0.01; **p<0.005; ***p<0.001
Standard errors are in parentheses and are clustered on state.
Probability is reported in percentage points.

Table S7. Food Safety Violations per Inspection, County Mean

	Dependent Variable: Mean Violations per Inspection	
	(1)	(2)
TMAX	−0.003	
	(0.002)	
TMAX²	0.0001***	
	(0.00004)	
HEAT INDEX		0.0001
		(0.001)
HEAT INDEX²		0.00003
		(0.00002)
PRCP	0.0003	0.0003
	(0.0003)	(0.0003)
TRANGE	−0.001	−0.001
	(0.001)	(0.001)
CLOUD	0.0002	0.0003**
	(0.0001)	(0.0001)
HUMID	0.001	
	(0.0003)	
WIND	−0.002**	−0.002**
	(0.001)	(0.001)
County FE	Yes	Yes
Date FE	Yes	Yes
State:Month FE	Yes	Yes
Observations	558,275	558,275
R^2	0.666	0.666
Adjusted R^2	0.663	0.663
Residual Std. Error	3.248	3.248

Note: *p<0.01; **p<0.005; ***p<0.001
Standard errors are in parentheses and are clustered on state.
Regressions are weighted by number of inspections per county.

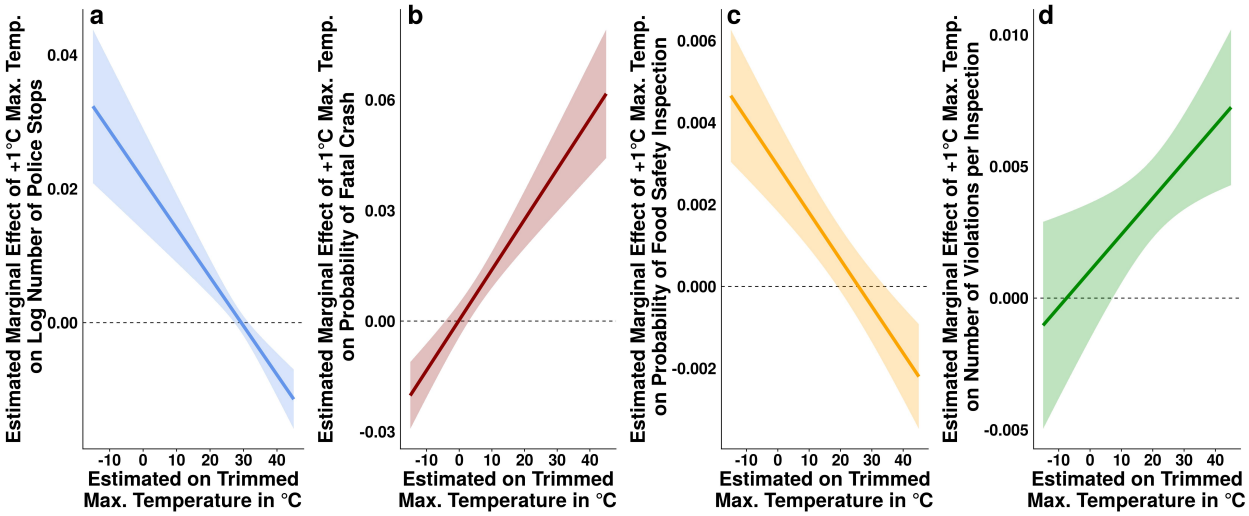

Fig. S6. Marginal effects and confidence intervals of quadratic estimates of trimmed maximum temperature regressions. This figure plots the marginal effects of the quadratic estimates from the trimmed maximum temperature distribution regressions. Panel (a) plots the marginal effect of a one degree increase in maximum temperature on the log number of police stops. Panel (b) plots the marginal effect of temperature on the probability of a fatal crash. Panel (c) plots the marginal effect of temperature on the probability of a food safety inspection. Panel (d) plots the marginal effect of temperature on the number of food safety violations per inspection. The marginal effects are plotted across the full distribution of temperature for comparability with the estimates from the main text regressions, even though these parameters are estimated on the constrained 2.5-97.5 percentiles of maximum temperatures. Shaded regions plot the 95% confidence intervals of the marginal effects.

(1, 16–19). While the binned functional forms we uncover in Fig. S3 assuage these concerns somewhat, another way to rule out undue influence is to omit the extreme values of the maximum temperature distribution and re-estimate our relationships on the trimmed maximum temperature distribution. As can be seen in Fig. S6 and Table S8, our results do not appear to be unduly leveraged by outliers on the temperature distribution.

Trimmed temperature marginal effects

Fig. S6 displays the marginal effects associated with the quadratic estimates from the trimmed maximum temperature distribution regressions. Each estimated relationship has substantial portions of its marginal effects' confidence intervals that do not contain zero. Of note, the negative marginal effects for the colder portion of the number of violations per inspection relationship are estimated with high uncertainty, while the higher temperature portion of the distribution returns positive marginal effects estimated with higher statistical precision. Of further note, we plot the marginal effects across the full distribution of temperature for comparison with the non-trimmed marginal effects plots in Fig. S2; the parameters, however, are estimated across the 2.5th to 97.5th percentile of maximum temperature for each relationship. For example, this maximum temperature range for the crash data is -5℃ to 35℃. Panel (a) of Fig. S6 draws from the estimates presented in model (1) of Table S8. Panel (b) of Fig. S6 draws from the estimates presented in model (2) of Table S8. Panel (c) of Fig. S6 draws from the estimates presented in model (3) of Table S8. Panel (d) of Fig. S6 draws from the estimates presented in model (4) of Table S8. As can be seen, the estimated relationships are robust to the exclusion of extreme portions of the maximum temperature distribution.

Table S8. Trimmed Maximum Temperature Regression Table

	Police Stops	Fatal Crashes	Food Safety Inspections	Food Safety Violations
	(1)	(2)	(3)	(4)
TMAX	0.019***	−0.008*	0.003***	0.002
	(0.004)	(0.003)	(0.001)	(0.002)
TMAX²	−0.0003***	0.001***	−0.0001***	0.0001
	(0.0001)	(0.0001)	(0.00001)	(0.00004)
PRCP	−0.012***	0.006***	−0.0003**	0.0003
	(0.001)	(0.001)	(0.0001)	(0.0004)
TRANGE	0.002	0.002	−0.0005	−0.002***
	(0.001)	(0.002)	(0.0005)	(0.001)
CLOUD	−0.002***	−0.001	−0.00001	0.0001
	(0.0003)	(0.0004)	(0.00003)	(0.0001)
HUMID	−0.001***	−0.002***	−0.0002	0.001*
	(0.0003)	(0.0004)	(0.0001)	(0.0002)
WIND	−0.004**	−0.010***	−0.001	−0.002**
	(0.001)	(0.002)	(0.001)	(0.001)
County FE	Yes	Yes	No	No
Facility FE	No	No	Yes	Yes
Date FE	Yes	Yes	Yes	Yes
State:Month FE	Yes	Yes	Yes	Yes
Observations	896,822	16,171,390	1,117,924,790	3,919,195
R^2	0.721	0.084	0.004	0.525
Adjusted R^2	0.719	0.083	0.003	0.412
Residual Std. Error	0.547	15.831	5.901	2.700

Note: *p<0.01; **p<0.005; ***p<0.001
Standard errors are in parentheses and are clustered on state.

Trimmed temperature regression table

Table S8 displays the results from estimating the main text models on the subset of the 2.5th to 97.5th percentile range of the maximum temperature distribution for each relationship. Fig. S6 displays the marginal effects and confidence bounds associated with these estimates.

Climate impact projections

Annualized projections, RCP4.5 emissions scenario

Here we replicate Figure 4 from the main text substituting the RCP4.5 emissions scenario (20) for the RCP8.5 emissions scenario employed in the main text. Fig. S7 depicts the results of these projections. As compared to the RCP8.5 scenario, the magnitude of our projected changes are smaller across the four outcome measures we investigate, though the general direction and spatial variation in the impacts remains similar to the projections presented in Figure 4 of the main text.

By-month grid-cell projections

RCP4.5 emissions scenario

Warming future temperatures – and thus any impact of climate change on regulatory behaviors and public safety risks – are likely to vary both spatially and temporally across the United States. How might the future impacts of warming on our regulatory and pubic safety outcome measures vary both geographically and temporally? To investigate this question, we take perform the projection from the main text Equations 2 and 3 for each month in the future years of 2050 and 2099 (9, 12). For the 2050 projection, we assign to each

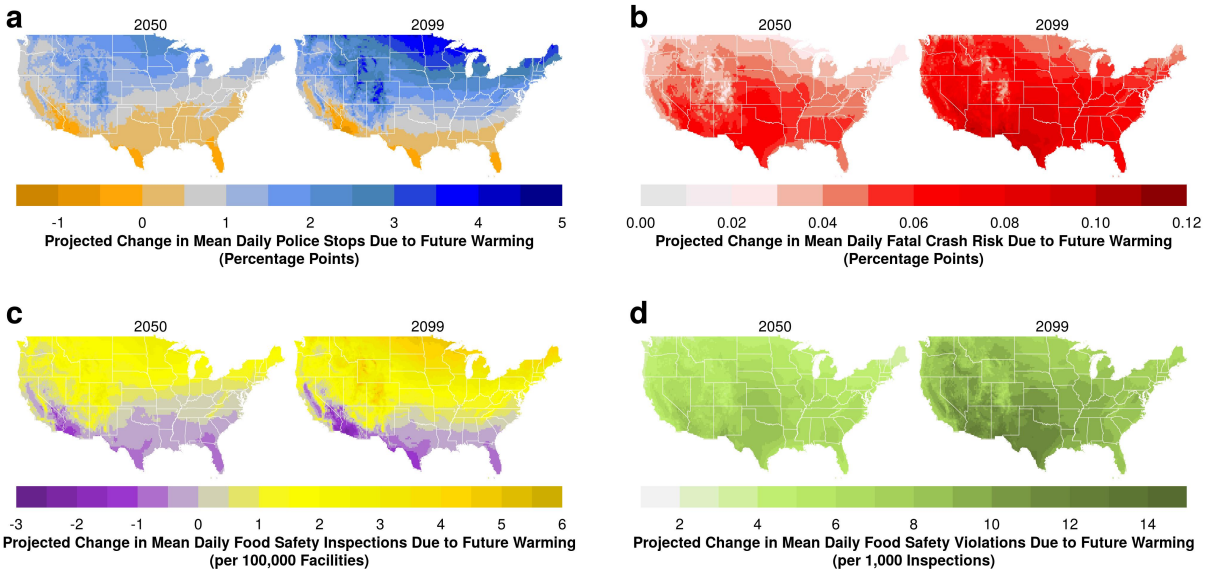

Fig. S7. Projected change in regulatory behaviors and outcomes in the US due to future warming. This figure presents the 25km x 25km grid cell projections of the effects of warming in the United States over this century on the regulatory outcomes examined in this study. Projections are calculated using downscaled climatic model data from NASA's NEX under the RCP4.5 emissions scenario (RCP8.5 projections presented in main text) across the mean of the 21 CMIP5 models in the ensemble. We couple these climate model data with the estimates from our historical statistical models to project the mean effects of climate change on each outcome. Panel (a) depicts projected changes to police stops, panel (b) depicts projected changes to fatal crash risk, panel (c) depicts projected changes to food safety inspections, and panel (d) depicts projected changes to food safety violations.

grid cell the projected net monthly difference in our outcome measure between 2010 and 2050. For the 2099 projection we assign to each grid cell the projected net monthly difference in our respective outcome measure between 2010 and 2099.

Employing the RCP4.5 emissions scenario, Fig. S8 shows the projected geographical differences in the effects of warming on police regulatory stops in the future. Fig. S9 shows the projected geographical differences in the effects of warming on fatal vehicular crashes. Fig. S10 shows the projected geographical differences in the effects of warming on food safety inspections. And Fig. S8 shows the projected geographical differences in the effects of warming on food safety violations. Across our projections, we observe that future climate change, particularly during summer months in the US south, may amplify the currently existing regulatory gaps between police stops and fatal crashes and food safety inspections and food safety violations.

RCP8.5 emissions scenario

Employing the RCP8.5 high emissions scenario, Fig. S12 shows the projected geographical differences in the effects of warming on police regulatory stops in the future. Fig. S13 shows the projected geographical differences in the effects of warming on fatal vehicular crashes. Fig. S14 shows the projected geographical differences in the effects of warming on food safety inspections. And Fig. S12 shows the projected geographical differences in the effects of warming on food safety violations. The projections that employ the RCP8.5 scenario find similar direction of impacts as those observed under the RCP4.5 scenario based projections, however the magnitude of the projected effects are larger due to the amplified temperature changes associated with the RCP8.5 scenario.

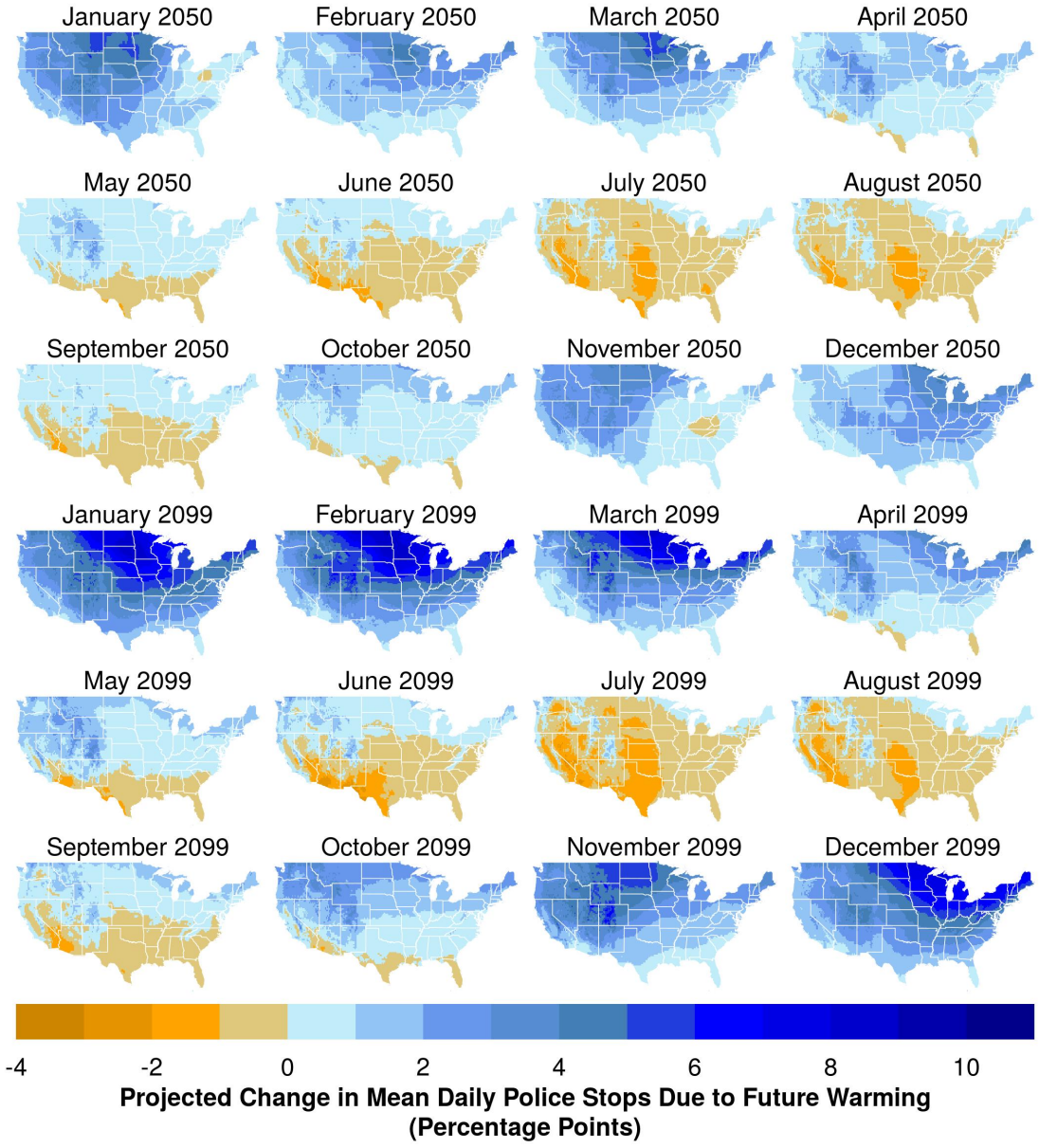

Fig. S8. Grid cell projections of change in number of police stops for RCP4.5. This figure presents the 25km x 25km grid cell projections of the potential impact of warming maximum temperatures on the percentage point change in police stops in future months. In this figure, downscaled climatic model maximum temperature projections are averaged across the 21 models in the ensemble and then coupled with our historical model parameters to produce an estimated percentage point change in police stops in each geographic location for the months of 2050 and 2099. Areas of the northern United States – where non-summer temperatures are currently coldest – may experience increases in net police regulatory activity due to future warming. However, southern portions of the U.S. may experience net reductions in police regulatory stops due to future warming.

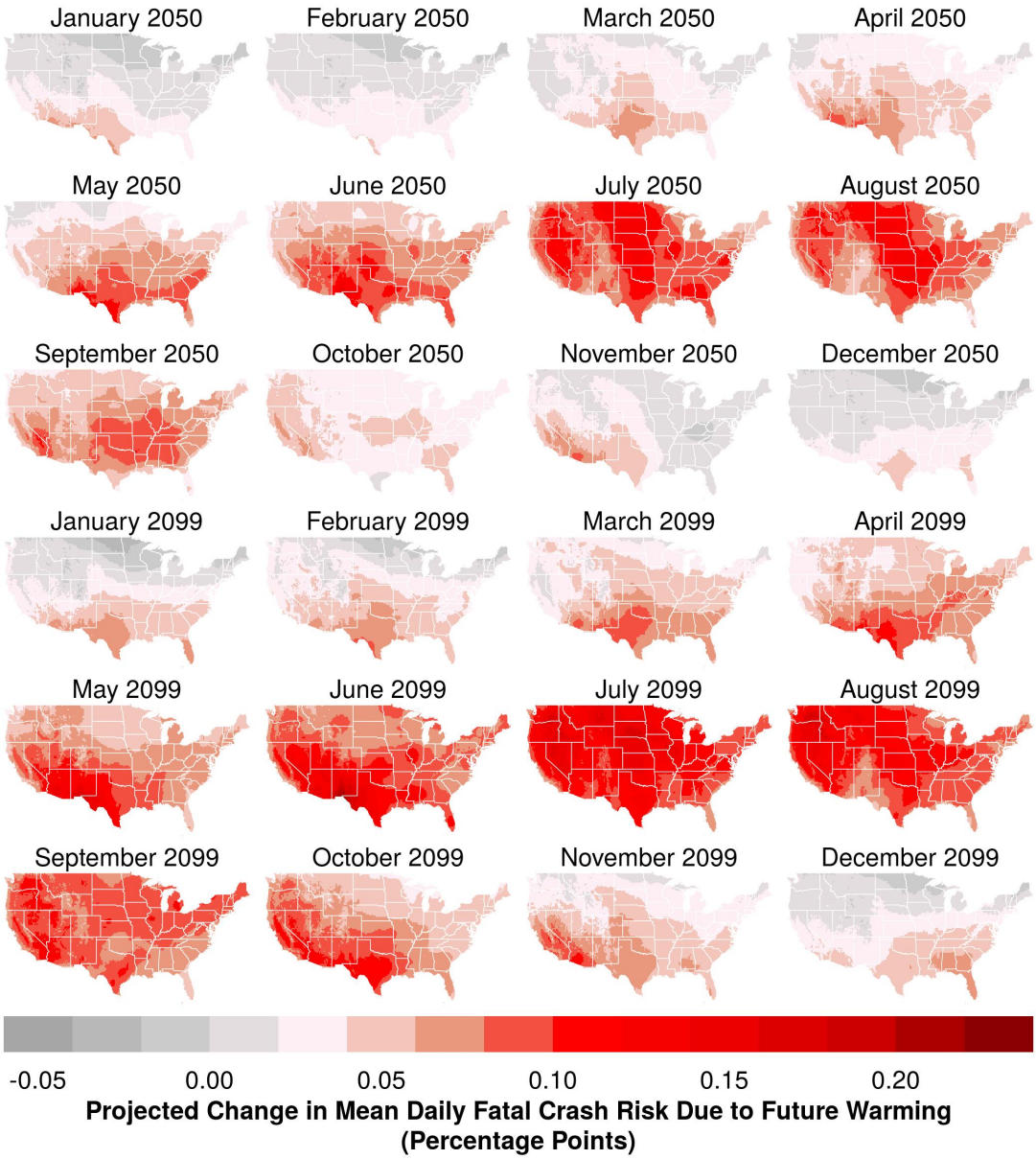

Fig. S9. Grid cell projections of change in number of fatal vehicular crashes for RCP4.5. This figure presents the 25km x 25km grid cell projections of the potential impact of warming maximum temperatures on the percentage point change in fatal crashes in future months. In this figure, downscaled climatic model maximum temperature projections are averaged across the 21 models in the ensemble and then coupled with our historical model parameters to produce an estimated percentage point change in fatal crashes in each geographic location for the months of 2050 and 2099. Areas of the northern United States – where non-summer temperatures are currently coldest – may experience decreases in net fatal crashes in the winter due to future warming. However, southern portions of the U.S. – especially in summer months – may experience net increases in fatal vehicular crashes due to future warming.

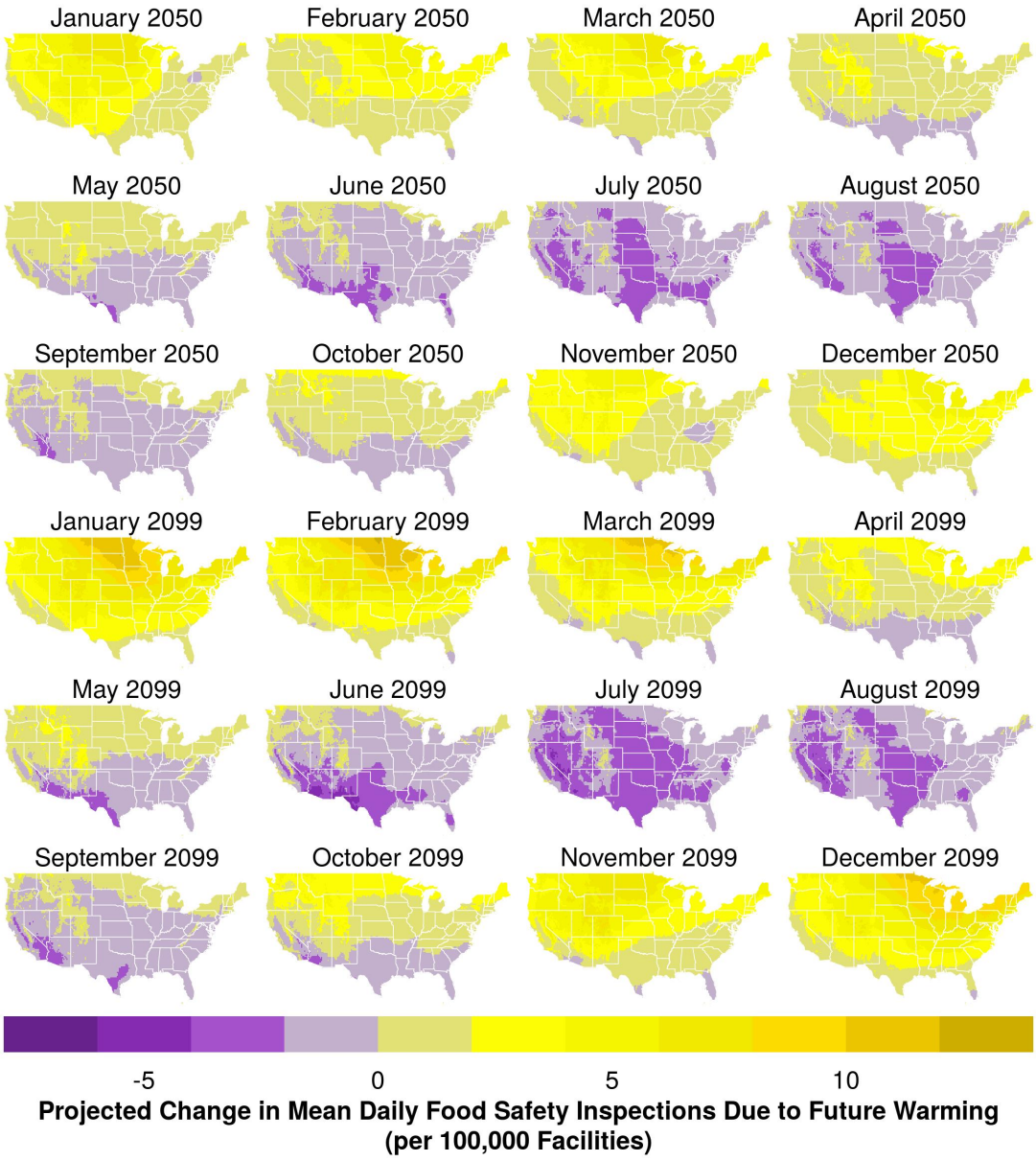

Fig. S10. Grid cell projections of change in food safety inspections for RCP4.5. This figure presents the 25km x 25km grid cell projections of the potential impact of warming maximum temperatures on the change in food safety regulatory inspections in future months. In this figure, downscaled climatic model maximum temperature projections are averaged across the 21 models in the ensemble and then coupled with our historical model parameters to produce an estimated change in food safety inspections per 1,000 facilities in each geographic location for the months of 2050 and 2099. Areas of the northern United States may experience increases in net food safety inspection activity during the winter months due to future warming. Southern portions of the U.S. may experience net reductions in inspection activity – particularly during summer months when food safety risks are highest – due to future warming.

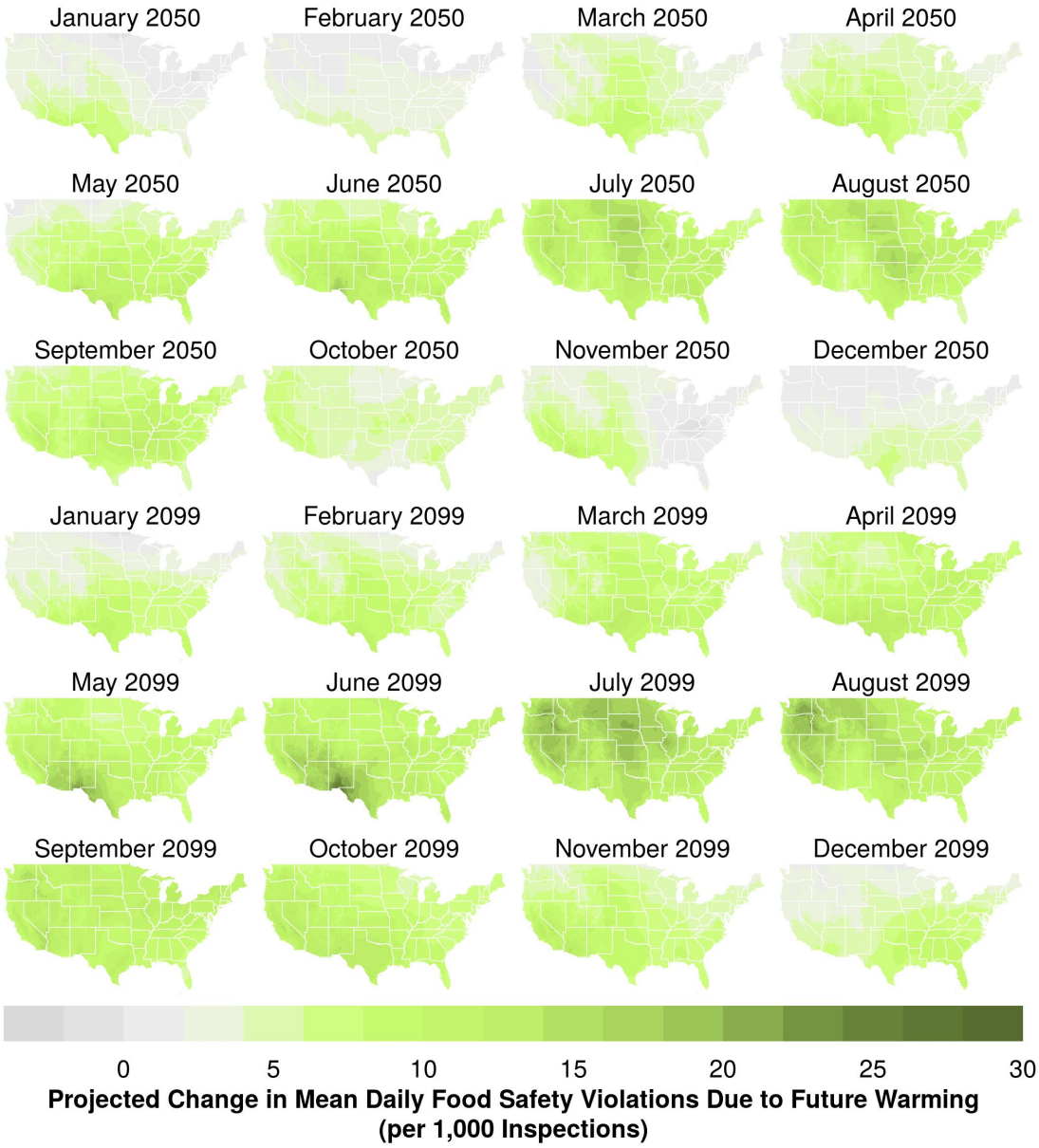

Fig. S11. Grid cell projections of change in number of food safety violations for RCP4.5. This figure presents the 25km x 25km grid cell projections of the potential impact of warming maximum temperatures on the change in food safety violations in future months. In this figure, downscaled climatic model maximum temperature projections are averaged across the 21 models in the ensemble and then coupled with our historical model parameters to produce an estimated change in food safety violations per 1,000 inspections for each geographic location for the months of 2050 and 2099. Our projection suggests that warming may increase food safety violation rates across the entire US by 2099.

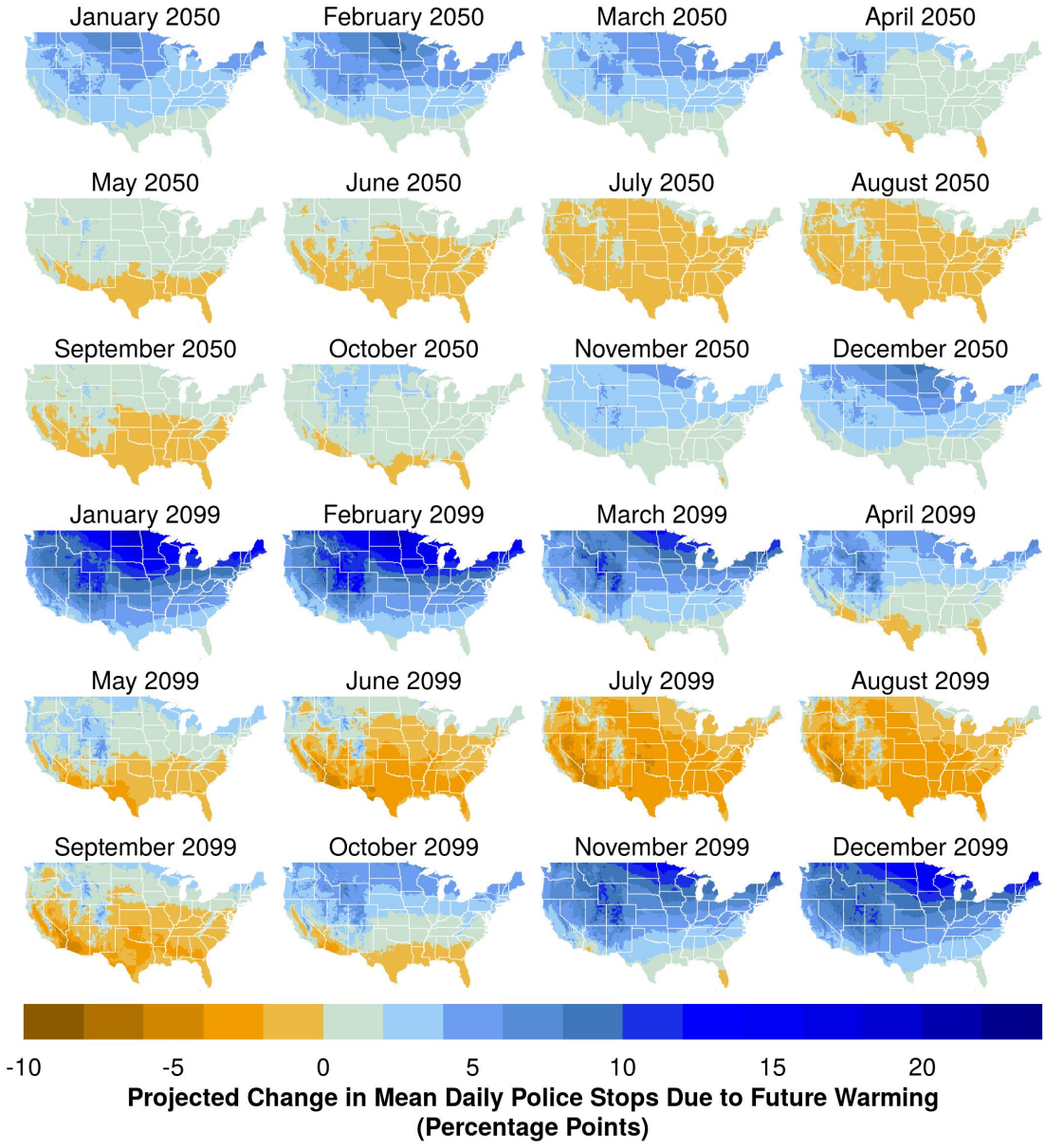

Fig. S12. Grid cell projections of change in number of police stops for RCP8.5. This figure presents the 25km x 25km grid cell projections of the potential impact of warming maximum temperatures on the percentage point change in police stops in future months. In this figure, downscaled climatic model maximum temperature projections are averaged across the 21 models in the ensemble and then coupled with our historical model parameters to produce an estimated percentage point change in police stops in each geographic location for the months of 2050 and 2099. Areas of the northern United States – where non-summer temperatures are currently coldest – may experience increases in net police regulatory activity due to future warming. However, southern portions of the U.S. may experience net reductions in police regulatory stops due to future warming.

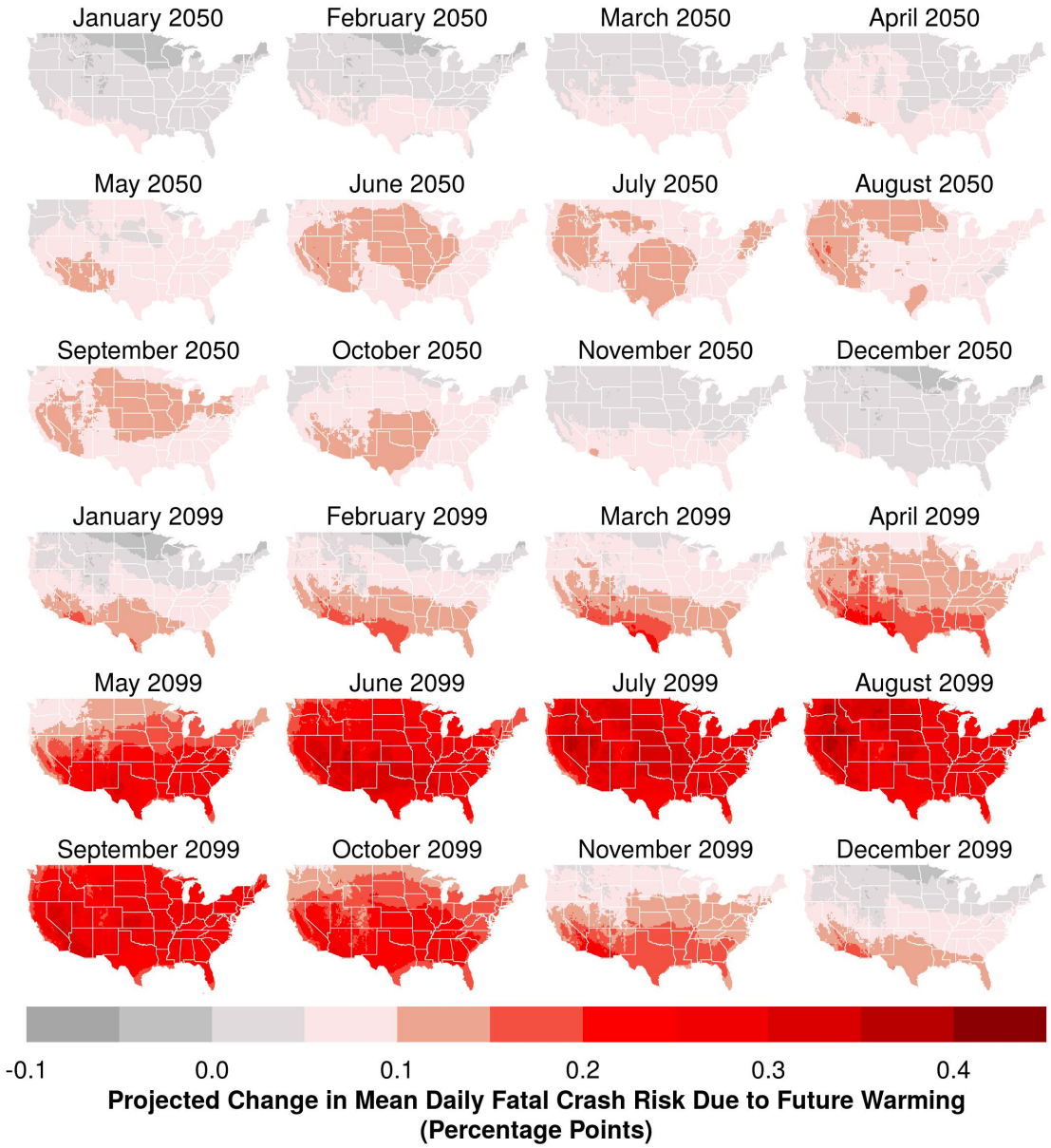

Fig. S13. Grid cell projections of change in number of fatal vehicular crashes for RCP8.5. This figure presents the 25km x 25km grid cell projections of the potential impact of warming maximum temperatures on the percentage point change in fatal crashes in future months. In this figure, downscaled climatic model maximum temperature projections are averaged across the 21 models in the ensemble and then coupled with our historical model parameters to produce an estimated percentage point change in fatal crashes in each geographic location for the months of 2050 and 2099. Areas of the northern United States – where non-summer temperatures are currently coldest – may experience decreases in net fatal crashes in the winter due to future warming. However, southern portions of the U.S. – especially in summer months – may experience net increases in fatal vehicular crashes due to future warming.

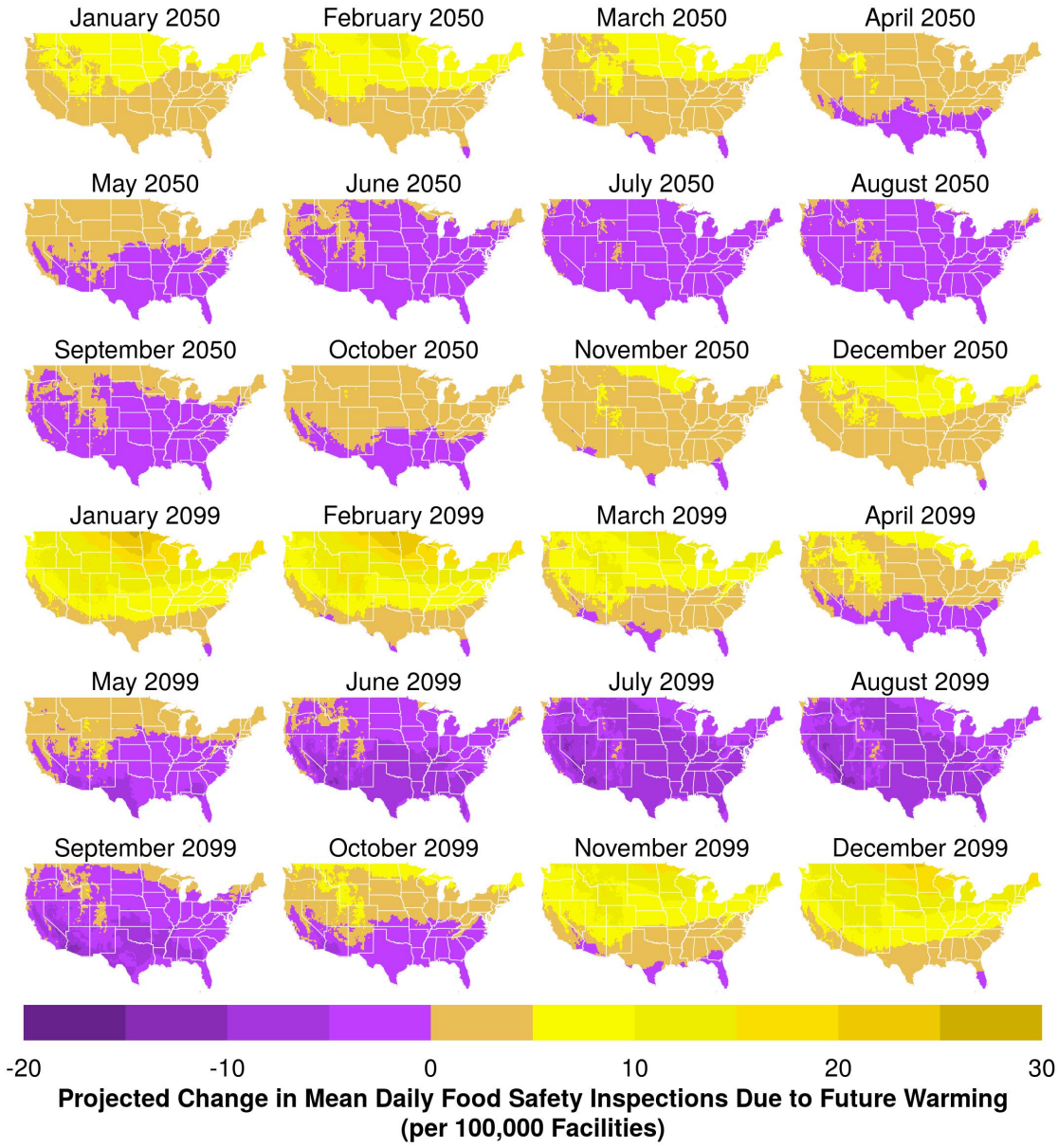

Fig. S14. Grid cell projections of change in food safety inspections for RCP8.5. This figure presents the 25km x 25km grid cell projections of the potential impact of warming maximum temperatures on the change in food safety regulatory inspections in future months. In this figure, downscaled climatic model maximum temperature projections are averaged across the 21 models in the ensemble and then coupled with our historical model parameters to produce an estimated change in food safety inspections per 1,000 facilities in each geographic location for the months of 2050 and 2099. Areas of the northern United States may experience increases in net food safety inspection activity during the winter months due to future warming. Southern portions of the U.S. may experience net reductions in inspection activity – particularly during summer months when food safety risks are highest – due to future warming.

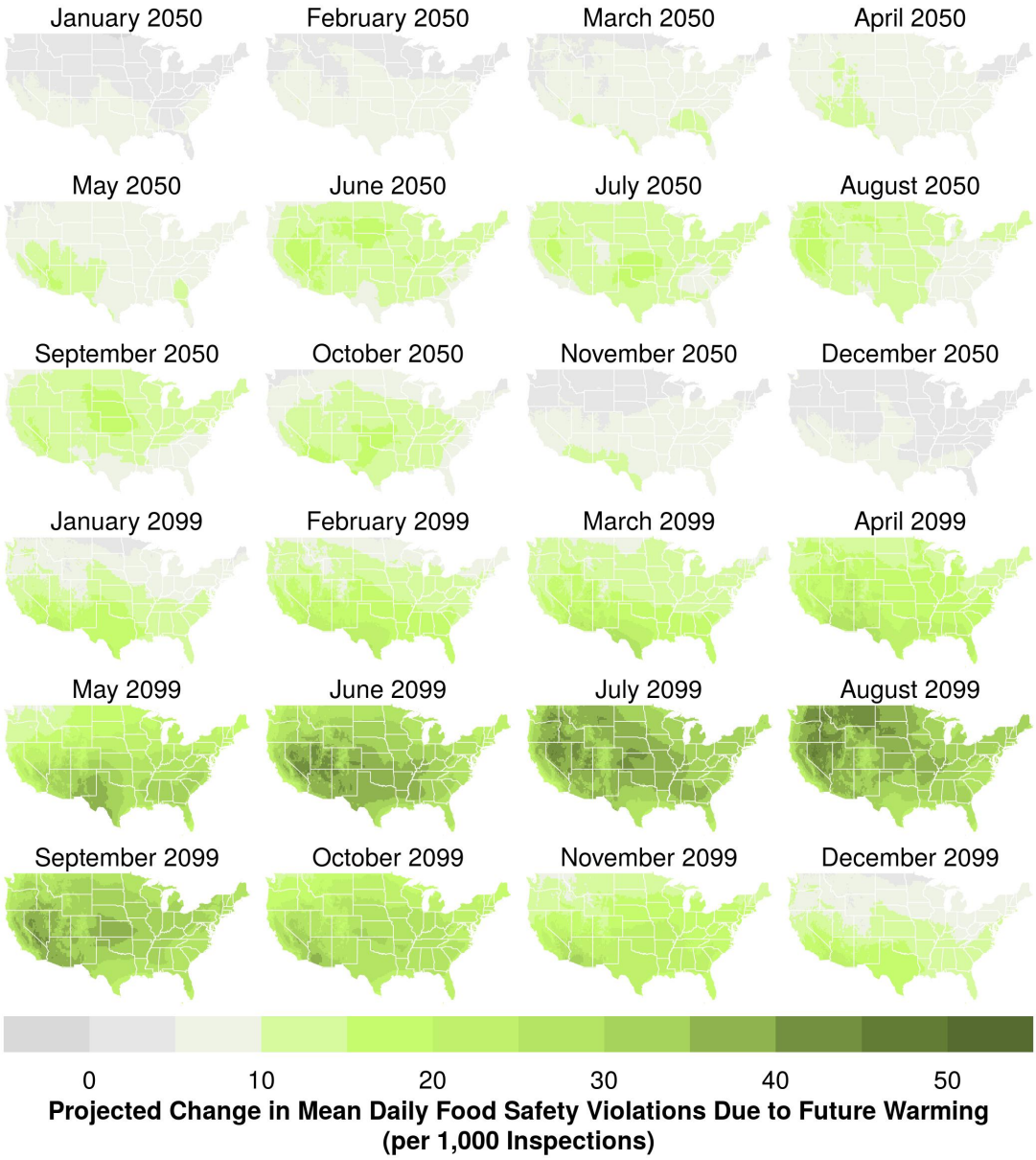

Fig. S15. Grid cell projections of change in number of food safety violations for RCP8.5. This figure presents the 25km x 25km grid cell projections of the potential impact of warming maximum temperatures on the change in food safety violations in future months. In this figure, downscaled climatic model maximum temperature projections are averaged across the 21 models in the ensemble and then coupled with our historical model parameters to produce an estimated change in food safety violations per 1,000 inspections for each geographic location for the months of 2050 and 2099. Our projection suggests that warming may increase food safety violation rates across the entire US by 2099.

References

1. Hsiang S (2016) Climate econometrics. *Annual Review of Resource Economics* 8(1):43–75.

2. Carleton TA, Hsiang SM (2016) Social and economic impacts of climate. *Science* 353(6304):aad9837.

3. Granger CW, Newbold P (1974) Spurious regressions in econometrics. *Journal of Econometrics* 2(2):111–120.

4. Berry WD, Golder M, Milton D (2012) Improving tests of theories positing interaction. *The Journal of Politics* 74(03):653–671.

5. Deschênes O, Greenstone M (2011) Climate change, mortality, and adaptation: Evidence from annual fluctuations in weather in the US. *American Economic Journal: Applied Economics* 3(4):152–185.

6. Ranson M (2014) Crime, weather, and climate change. *Journal of Environmental Economics and Management* 67(3):274–302.

7. Graff Zivin JS, Neidell M (2014) Temperature and the allocation of time: Implications for climate change. *Journal of Labor Economics* 32(1):1–26.

8. Obradovich N (2017) Climate change may speed democratic turnover. *Climatic Change* 140(2):135–147.

9. Obradovich N, Fowler JH (2017) Climate change may alter human physical activity patterns. *Nature Human Behaviour* 1:0097.

10. Baylis P, et al. (2018) Weather impacts expressed sentiment. *PloS one* 13(4):e0195750.

11. Miller TR, Blincoe LJ (1994) Incidence and cost of alcohol-involved crashes in the United States. *Accident Analysis & Prevention* 26(5):583–591.

12. Obradovich N, Migliorini R, Mednick SC, Fowler JH (2017) Nighttime temperature and human sleep loss in a changing climate. *Science Advances* 3(5):e1601555.

13. Hancock PA, Ross JM, Szalma JL (2007) A meta-analysis of performance response under thermal stressors. *Human Factors* 49(5):851–877.

14. Steadman RG (1979) The assessment of sultriness. part I: A temperature-humidity index based on human physiology and clothing science. *Journal of Applied Meteorology* 18(7):861–873.

15. Rothfusz LP (1990) The heat index equation (or, more than you ever wanted to know about heat index). *Fort Worth, Texas: National Oceanic and Atmospheric Administration, National Weather Service, Office of Meteorology* 9023.

16. Auffhammer M, Hsiang SM, Schlenker W, Sobel A (2013) Using weather data and climate model output in economic analyses of climate change. *Review of Environmental Economics and Policy*:ret016.

17. Dell M, Jones BF, Olken BA (2014) What do we learn from the weather? The new climate-economy literature. *Journal of Economic Literature* 52(3):740–798.

18. Greene WH (2003) *Econometric analysis* (Pearson Education).

19. Wooldridge JM (2010) *Econometric analysis of cross section and panel data* (MIT press).

20. Thomson AM, et al. (2011) RCP4. 5: A pathway for stabilization of radiative forcing by 2100. *Climatic change* 109(1-2):77.